Arbeiten werden in dieser Richtung weitergeführt. Abschätzungen ergeben, daß die Breite von Schwingungen, die Verbreiterungen der hier behandelten Art zeigen, bei unendlicher Verdünnung auf Werte in der Größenordnung von 1 cm^{-1} zurückgehen. Das ist aber auch die Größenordnung, die voll polare Banden, die keine Temperatur- und Konzentrationsabhängigkeit zeigen, aufweisen. Im Falle des Thiophens ist das näherungsweise erfüllt für ν_4. ν_8 ist zwar breiter, zeigt aber ebenfalls keine Temperatur- und Konzentrationsabhängigkeit. Die Ursache für ein solches Verhalten der beiden Normalschwingungen wird offenbar, wenn man beachtet, daß das Übergangsmoment für die hier behandelten Vorgänge proportional dem Quadrat der Ableitung des Dipolmomentes μ nach der entsprechenden Normalkoordinate Q_i ist. Aus der Tatsache, daß die IR-Intensität der beiden Normalschwingungen sehr schwach ist, ergibt sich, daß die Größe $(\partial\mu/\partial Q_i)^2$ sehr klein ist. Alle anderen untersuchten Schwingungen ν_3, ν_5, ν_6, ν_7 zeigen Verbreiterung, wenn die Substanz in hoher Konzentration vorliegt. Die stärksten Effekte sind bei ν_5 und ν_6 beobachtet worden. Auf diese beiden Schwingungen, die beide unter Veränderung des Abstandes der beiden „Doppelbindungen" ablaufen, wurde deshalb der Hauptteil der Untersuchungen konzentriert.

Herrn Prof. Dr. CORDES bin ich sowohl für die Überlassung der zur Durchführung der Arbeiten notwendigen Geräte, als auch für die diese Arbeit fördernden Diskussionen zu großem Dank verpflichtet. — Die Untersuchungen wurden ermöglicht durch Sachbeihilfen der Deutschen Forschungsgemeinschaft und der Stiftung Volkswagenwerk.

Numerical Solution for the Forward Steady-State Behaviour of an Abrupt p^+-n Junction

M. SÁNCHEZ

Institut für höhere Elektrotechnik der Eidgenössischen Technischen Hochschule Zürich

(Z. Naturforsch. **23 a**, 1135—1146 [1968]; received 8 April 1968)

The forward steady-state behaviour of a one-dimensional abrupt p^+-n junction germanium diode at zero and at low to high injection levels is analysed. For this purpose the numerical integration of the current differential equations, the continuity equations, and Poisson's differential equation is performed not only inside the space-charge layer but also along the quasineutral regions of the diode satisfying the boundary and continuity conditions. The integration is made on a digital computer without applying the Boltzmann equilibrium approximation in the space-charge layer and the space-charge neutrality approximation in the quasineutral regions. Furthermore, the acoustical and optical mode scattering, the ionized impurity scattering, and the Hall-Shockley-Read and Auger recombination processes are included in the calculation. The method of solution applied differs from those already available in the literature and permits the "exact" computation of the space-charge density inside the relatively long (compared with the Debye length) quasineutral p and n regions of the diode considered. The numerical results for the hole and electron concentration distributions, the electric field distributions, the electron current density distributions, the electrostatic potential distributions and the space-charge density distributions are reported for five values of the total current density across the p-n junction. The comparison of the obtained numerical solutions with the closed analytical solutions for zero bias (as a test of the computer program) on the one side and of the computed current/voltage characteristic of the p-n junction with experimental values on the other side shows satisfactory agreement.

The theory of a one-dimensional p-n junction diode [1] under steady-state conditions leads to a boundary-value problem with an autonomous system of nonlinear ordinary differential equations, when the Boltzmann equilibrium approximation in the space-charge layer and the space-charge neutrality approximation in the quasineutral regions of the diode are not applied. Since a general closed analytical solution of this system does not exist, numerical methods have to be used to obtain solutions which are not restricted by simplifying assumptions. However, a difficulty arises here, since, with these equations,

[1] W. SHOCKLEY, Bell Syst. Tech. J. **28**, 435 [1949].

the solutions obtained by numerical integration of the trajectories diverge rapidly from the desired solutions [2].

In order to avoid such difficulty an iteration scheme, suitable for solution by digital computers, has been presented for a one-dimensional transistor [3] by converting Poisson's equation into a system of difference equations and using the electrostatic potential and the hole and electron quasi-Fermi potentials as dependent variables. However, another difficulty arises by applying this method, since, by inserting the values of the dependent variables into Poisson's equation, the space-charge density becomes equal to a relatively small difference between nearly equal numbers in the quasineutral regions of the devices. At the space-charge layer boundaries of the p-n junction considered in this paper as an example, the net space-charge density is 10^6 and 10^{17} times smaller than the doping of the quasineutral n and p regions respectively, for a current density of 10^2 mA/cm^2 (see Fig. 13 and 9). Therefore, for the device considered here, the relative error of the values of the dependent variables computed with the method in Ref. [3] must be smaller than 10^{-6} and 10^{-17} respectively. This seems practically impossible to attain.

In order to avoid the two above difficulties a method for the numerical solution of the boundary-value problem of a p-n junction diode is presented here, which differs from those already available in the literature and permits the "exact" computation of the space-charge density in the quasineutral regions of the diode without applying the mentioned approximations. Some distinctive features of the present method are the following:

(a) reduction of the boundary-value problem to an initial-value problem by numerical integration of the characteristics [4] of the system of differential equations, rather than the trajectories;

(b) performance of the numerical integration from each external contact of the p-n junction towards the transition of the doping profile;

(c) use of the space-charge density as a dependent variable in the quasineutral regions of the p-n junction.

With the present method a computer solution has been obtained for the forward steady-state behaviour of a one-dimensional abrupt p^+-n junction germanium diode of relatively long quasineutral regions at zero and at low to high injection levels, by taking into account the Hall-Shockley-Read and the Auger recombination processes.

After a preliminary account [5] of some of the present work appeared, two further treatments [6, 7] of the boundary-value problem have been published with results obtained by neglecting the influence of the recombination processes.

1. Boundary-Value Problem

To describe the forward steady-state behaviour of the one-dimensional p-n junction, the five equations to be solved are [8–12]:

$$J_p = e\,p\,\mu_p\,E - e\,D_p\frac{dp}{dx}, \tag{1}$$

$$J_n = e\,n\,\mu_n\,E + e\,D_n\frac{dn}{dx}, \tag{2}$$

$$\frac{dJ_p}{dx} = -e\,R, \tag{3}$$

$$\frac{dJ_n}{dx} = e\,R, \tag{4}$$

$$\frac{dE}{dx} = \frac{e}{\varepsilon}\,(p - n + n_D - n_A), \tag{5}$$

where

J_p, J_n = hole and electron current densities,
e = electronic charge,
p, n = hole and electron concentrations,
μ_p, μ_n = hole and electron mobilities,
E = electric field,
D_p, D_n = hole and electron diffusion constants,
R = recombination rate,
ε = permittivity,
n_D, n_A = donor and acceptor concentrations.

[2] S. P. Morgan and F. M. Smits, Bell Syst. Tech. J. **39**, 1573 [1960].
[3] H. K. Gummel, IEEE Trans. Electron Devices **ED-11**, 455 [1964].
[4] L. Bieberbach, Einführung in die Theorie der Differentialgleichungen im reellen Gebiet, Springer, Berlin 1956.
[5] M. Sánchez, Electron. Letters **3**, 117, 160, 223 [1967].
[6] A. De Mari, Solid-State Electron. **11**, 33 [1968].
[7] V. Arandjelović and J. J. Sparkes, Electron. Letters **3**, 357 [1967].
[8] M. Sánchez, Helv. Phys. Acta **36**, 1 [1963].
[9] W. Shockley and W. T. Read, Phys. Rev. **87**, 835 [1952].
[10] R. N. Hall, Phys. Rev. **87**, 387 [1952].
[11] R. N. Hall, Proc. IEE, **106 B**, Suppl. 15–18, 923 [1959].
[12] D. A. Evans and P. T. Landsberg, Solid-State Electron. **6**, 169 [1963].

A closed integral of the differential equations system (1) – (5) is:

$$J = J_p + J_n , \tag{6}$$

where the total current density J is independent of x.

The recombination mechanisms to be considered are the Hall-Shockley-Read and the Auger processes. Thus

$$R = \frac{p\,n - n_i^2}{\tau_{p0}(n+n_1)+\tau_{n0}(p+p_1)} , \tag{7}$$

with

$$\tau_{n0} = \frac{1}{M(B_p+\beta_{nn}\,n+\beta_{np}\,p)} , \tag{8}$$

$$\tau_{p0} = \frac{1}{M(B_n+\beta_{pn}\,n+\beta_{pp}\,p)} , \tag{9}$$

$$n_1 = n_i \exp\{(E_t - E_i)/k\,T\} , \tag{10}$$

$$p_1\,n_1 = n_i^2 , \tag{11}$$

where

n_i = electron concentration in an intrinsic specimen,
M = concentration of traps,
$B_p, B_n, \beta_{nn}, \beta_{pn}, \beta_{np}, \beta_{pp}$ = recombination coefficients,
E_t = energy level of the traps,
E_i = intrinsic Fermi level,
k = Boltzmann's constant,
T = absolute temperature.

The doping profile of the p-n junction germanium diode is taken as

$n_A = 10^{18}/\mathrm{cm}^3$, $n_D = 0$ for $0 \leqq x < 20\ \mu\mathrm{m}$,

$n_A = 0$, $n_D = 4.6 \times 10^{14}/\mathrm{cm}^3$ for $20\ \mu\mathrm{m} \leqq x \leqq 40\ \mu\mathrm{m}$.

The values [11, 13–15] used are

$$\left.\begin{aligned} 1/M\,B_p &= 50\ \mu\mathrm{s},\\ \mu_p &= 657\ \mathrm{cm}^2/\mathrm{Vs},\\ 1/M\,B_n &= 5\ \mu\mathrm{s},\\ \mu_n &= 1102\ \mathrm{cm}^2/\mathrm{Vs} \end{aligned}\right\} \quad \text{for } 0 \leqq x < 20\ \mu\mathrm{m},$$

$$\left.\begin{aligned} 1/M\,B_p &= 500\ \mu\mathrm{s},\\ \mu_p &= 1793\ \mathrm{cm}^2/\mathrm{Vs},\\ 1/M\,B_n &= 50\ \mu\mathrm{s},\\ \mu_n &= 3750\ \mathrm{cm}^2/\mathrm{Vs} \end{aligned}\right\} \quad \text{for } 20\ \mu\mathrm{m} \leqq x \leqq 40\ \mu\mathrm{m},$$

$$\left.\begin{aligned} &B_p/\beta_{np} = 2\times 10^{17}/\mathrm{cm}^3,\\ &B_n/\beta_{pn} = 10^{17}/\mathrm{cm}^3,\\ &\beta_{nn} = \beta_{pp} = 0,\\ &E_t - E_i = -0.054\ \mathrm{eV},\\ &D_p = k\,T\,\mu_p/e,\ D_n = k\,T\,\mu_n/e,\\ &T = 300\ ^\circ\mathrm{K} \end{aligned}\right\} \quad \text{for } 0 \leqq x \leqq 40\ \mu\mathrm{m}.$$

The following boundary and continuity conditions are applied at the points representing the contacts and at the abrupt transition of the doping profile respectively:

$$\left.\begin{aligned} &p\,n = n_i^2,\\ &p - n + n_D - n_A = 0 \end{aligned}\right\} \quad \text{at } x = 0 \text{ and } x = 40\ \mu\mathrm{m},$$

$J_p(x)$, $J_n(x)$, $p(x)$, $n(x)$ and $E(x)$ are continuous at $x = 20\ \mu\mathrm{m}$.

With this formulation of the problem, the internal distributions of n, p, J_n, J_p and E and the terminal voltage of the p^+-n junction are determined for a given value of J.

2. Method of Solution

In order to solve the boundary-value problem of the abrupt p^+-n junction germanium diode considered, the following variables are introduced for the n region:

$$\begin{aligned} y_1 &= p - p_n , & y_2 &= n - n_n ,\\ y_3 &= J_p - J_{pn} , & y_4 &= E - E_n , \end{aligned} \tag{12}$$

$$V = -U , \qquad X = -x , \tag{13}$$

where the asymptotic values p_n, n_n, J_{pn} and E_n of p, n, J_p and E in a infinitely long n region are defined by

$$\left.\begin{aligned} J - J_{pn} - e\,n_n\,\mu_n\,E_n &= 0 ,\\ e\,p_n\,\mu_p\,E_n - J_{pn} &= 0 ,\\ p_n\,n_n - n_i^2 &= 0 ,\\ p_n - n_n + n_D &= 0 \end{aligned}\right\} \tag{14}$$

and U is the electrostatic potential.

y_1, y_2, y_3 and y_4 are then the excess asymptotic values of p, n, J_p and E.

By applying Eqs. (12) – (14) to the autonomous system of differential Eqs. (1), (2), (3), (5) and (6) of the trajectories, the following system of differential equations of the characteristics [4] as well as the differential equations for V and X is obtained:

$$\frac{dy_2}{dy_1} = \frac{\mu_p}{\mu_n}\frac{1}{y_3^*}\,(e\,\mu_n\,E_n\,y_2 + y_3 + e\,\mu_n\,n_n\,y_4 + e\,\mu_n\,y_2\,y_4), \tag{15}$$

$$\frac{dy_3}{dy_1} = e\,k\,T\,\mu_p\,\frac{1}{y_3^*}\,\frac{n_n\,y_1 + p_n\,y_2 + y_1\,y_2}{\tau_{n0}(p_n+p_1+y_1)+\tau_{p0}(n_n+n_1+y_2)} , \tag{16}$$

[13] J. A. Burton, G. W. Hull, F. J. Morin, and J. C. Severiens, J. Phys. Chem. **57**, 853 [1953].
[14] I. V. Karpova and S. G. Kalashnikov, Intern. Conf. Physics of Semiconductors, Exeter 1962, p. 880.
[15] M. Sánchez, Solid-State Electron. **6**, 183 [1963].

$$\frac{dy_4}{dy_1} = \frac{e}{\varepsilon} k T \mu_p \frac{1}{y_3^*} (-y_1 + y_2), \quad (17)$$

$$\frac{dV}{dy_1} = k T \mu_p \frac{1}{y_3^*} (-E_n - y_4), \quad (18)$$

$$\frac{dX}{dy_1} = k T \mu_p \frac{1}{y_3^*}, \quad (19)$$

where y_1 is the independent variable and

$$y_3^* = y_3 - e \mu_p p_n y_4 - e \mu_p y_1 (E_n + y_4). \quad (20)$$

For $0 \leqq y_1 \leqq 2 y_2$, Eq. (15) is rewritten

$$\frac{d(-y_1+y_2)}{dy_1} = \frac{\mu_p}{\mu_n} \frac{1}{y_3^*} \left\{ \left(1 - \frac{\mu_n}{\mu_p}\right) y_3 + e \mu_n (p_n + n_n)\, y_4 + e \mu_n (y_1 + y_2)\, (E_n + y_4) \right\} \quad (21)$$

and $(-y_1 + y_2) = -(p - n + n_D)$ replaces y_2 as dependent variable. For the p region, corresponding differential equations are obtained with the excess asymptotic value of n as independent variable, and with the following dependent variables: either $(p - n - n_A)$ or the excess asymptotic value of p, the excess asymptotic value of J_n, the excess asymptotic value of E, U and x.

The method of solution used consists of integrating numerically the system of differential Eqs. (21), (16), (17), (18) and (19) [with $(-y_1 + y_2)$ as dependent variable instead of y_2] from $y_1 = 0$ at $x = 40\ \mu$m to $y_1 = 2 y_2$ at a value of x between 40 μm and 20 μm, by using as initial values of $(-y_1 + y_2)$, y_3, y_4, V and X at $y_1 = 0$ the values obtained from the equations $-y_1 + y_2 = 0$, (19), (20), (21), $V = C^*$ and $X = -40\ \mu$m for $y_1 = 0$,

$$\frac{dX}{dy_1} = -1 \Big/ \left.\frac{dp}{dx}\right|_{x = 40\ \mu m}$$

and

$$\frac{d(-y_1+y_2)}{dy_1} = -1 + \frac{\left.dn/dx\right|_{x = 40\ \mu m}}{\left.dp/dx\right|_{x = 40\ \mu m}}$$

with C^* as a constant of integration and two guesses of the unknown initial values $\left.dp/dx\right|_{x = 40\ \mu m}$ and $\left.dn/dx\right|_{x = 40\ \mu m}$. Subsequently, the system of differential Eqs. (15), (16), (17), (18) and (19) (with y_2 as dependent variable) is then integrated numerically from $y_1 = 2 y_2$ to $y_1 = y_{1\,ab}$ at $x = 20\ \mu$m, by using as initial values the final values of the preceding integration. This process is repeated in the n region for various guesses of $\left.dp/dx\right|_{x = 40\ \mu m}$ and $\left.dn/dx\right|_{x = 40\ \mu m}$ and in the p region with the corresponding differential equations for various guesses of $\left.dn/dx\right|_{x = 0}$ and $\left.dp/dx\right|_{x = 0}$ until the values of n, p, E and J_n of the n and p side integrations become equal at $x = 20\ \mu$m (see appendix).

The computer program used [16] makes use of the procedure RK [17, 18] (adequately adapted to these initial-value problem calculations) which integrates the system of differential equations with the method of Runge-Kutta with automatic search for appropriate length of integration step.

By applying the procedure RK, the relative discretisation error of each integration step is smaller than a prefixed limit. This limit was 10^{-5} for all calculations made to obtain the results described in the following section. The calculations were performed on the Control Data 1604-A digital computer of the Computer Center of the Swiss Federal Institute of Technology in Zürich.

3. Numerical Results

With the described method, a computer solution of the boundary-value problem was obtained for the following values of J: 0, 10^2, 10^3, 10^4 and 4×10^4 mA/cm^2.

The calculated hole and electron concentrations p and n as a function of x in the Ge p$^+$-n junction diode are displayed in Figs. 1 – 4 with J as parameter. The values of p obtained from $x = 0$ to $x = 19.85\ \mu$m were 10^{18}/cm$^3 + \Delta p$ with $|\Delta p| < 4 \times 10^{13}$/cm^3. The values of p obtained at $x = 20\ \mu$m are given in Table 1.

Figs. 5 – 7 show the calculated electric field E as a function of x in the Ge p$^+$-n junction diode with J as parameter. The values of E obtained from $x = 0$ to $x = 19.85\ \mu$m were the values at $x = 19.85\ \mu$m with very small variations.

The values of E obtained at $x = 20\ \mu$m are given in Table 2.

The calculated electron current density J_n as a function of x in the Ge p$^+$-n junction diode is illustrated in Fig. 8 with J as parameter and K as a dimensionless factor.

Figs. 9 – 13 show the calculated net charge density $\varrho/e\,(= p - n + n_D - n_A)$ or $-\varrho/e$ as a function of x in the Ge p$^+$-n junction diode with J as parameter. The p and n side values of ϱ/e obtained at $x = 20\ \mu$m are given in Table 3.

[16] M. SÁNCHEZ, Stationäre Transportvorgänge in inhomogenen Halbleitern, Dissertation Nr. 4030, E.T.H. Zürich 1967.

[17] H. RUTISHAUSER, Programmgesteuertes Rechnen, Vorlesung E.T.H. Zürich 1957-58.

[18] P. NAUR et al., Numer. Math. **4**, 420 [1963].

J [mA/cm²]	0	10^2	10^3	10^4	4×10^4
p [cm^{-3}]	3.659×10^{17}	3.662×10^{17}	3.668×10^{17}	3.683×10^{17}	3.717×10^{17}

Table 1. p for $x=20$ μm.

J [mA/cm²]	0	10^2	10^3	10^4	4×10^4
E [V/cm]	-4.657×10^4	-4.653×10^4	-4.648×10^4	-4.630×10^4	-4.595×10^4

Table 2. E for $x=20$ μm.

J [mA/cm²]	0	10^2	10^3	10^4	4×10^4
ϱ/e [cm^{-3}] p side	-6.341×10^{17}	-6.338×10^{17}	-6.332×10^{17}	-6.317×10^{17}	-6.284×10^{17}
ϱ/e [cm^{-3}] n side	3.663×10^{17}	3.666×10^{17}	3.672×10^{17}	3.687×10^{17}	3.720×10^{17}

Table 3. p and n side values of ϱ/e for $x=20$ μm.

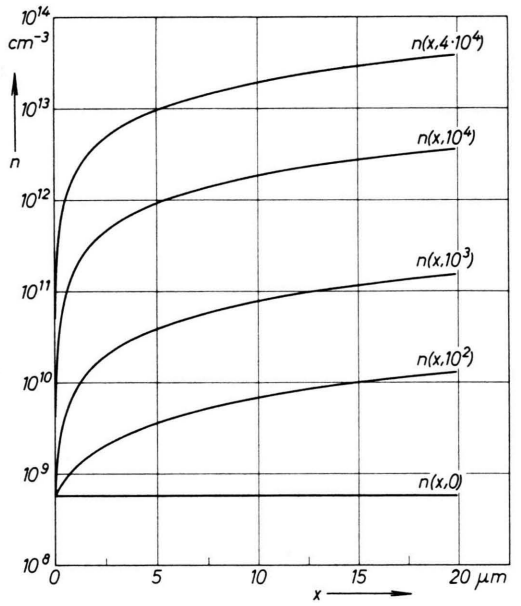

Fig. 1. Electron concentration distributions in the quasi-neutral p region of Ge p^+-n junction diode with total current density as parameter in mA/cm².

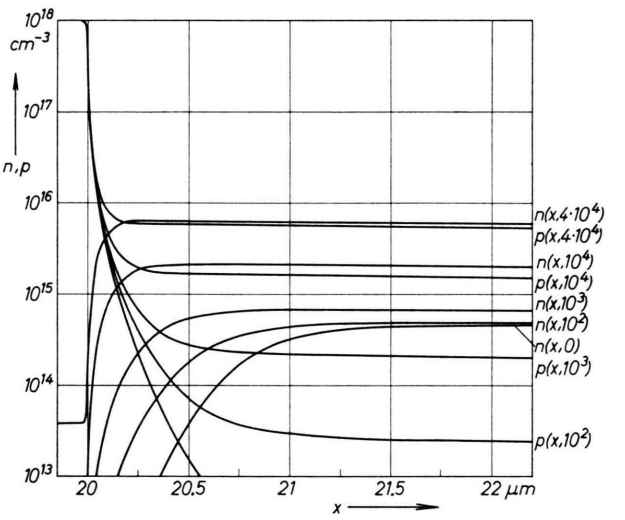

Fig. 2. Hole and electron concentration distributions in the space-charge layer of Ge p^+-n junction diode, for values larger than 10^{13}/cm³, with total current density as parameter in mA/cm².

Figs. 14 and 15 show the calculated electrostatic potential U as a function of x in the Ge p^+-n junction diode with J as parameter. The values of U obtained from $x=0$ to $x=19.85$ μm were $0+\Delta U$ with $|\Delta U|<7.6\times10^{-4}$ V. From these electrostatic potential distributions, the current/voltage characteristic of the p-n junction was obtained as illustrated in Fig. 16 (full curve), where U_K is the voltage at the terminals of the diode.

4. Comparison with Experiment

Fig. 16 shows the calculated forward d.c. total current density (full curve) across the one-dimensional abrupt p^+-n junction germanium diode as a function of eU_K/kT. The slope of the computed characteristic agrees for $J=10^2$ mA/cm² (low injection level) with the measured slope [19, 20] of the

[19] F. S. Goucher, G. L. Pearson, M. Sparks, G. K. Teal, and W. Shockley, Phys. Rev. **81**, 637 [1951].

[20] M. J. O. Strutt, Semiconductor Devices, Vol. 1, Academic Press, New York 1966.

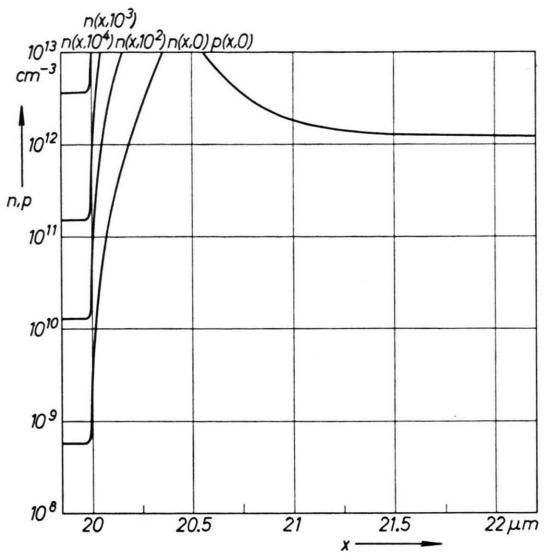

Fig. 3. Hole and electron concentration distributions in the space-charge layer of Ge p^+-n junction diode, for values smaller than $10^{13}/cm^3$, with total current density as parameter in mA/cm².

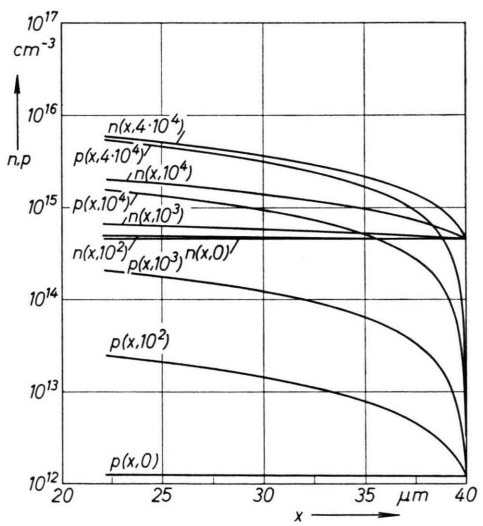

Fig. 4. Hole and electron concentration distributions in the quasineutral n region of Ge p^+-n junction diode with total current density as parameter in mA/cm².

(steeper broken) curve

$$J = \frac{10^2}{21.458}\left\{\exp\frac{e\,U_K}{k\,T} - 1\right\}\ \mathrm{mA/cm^2},$$

and also agrees for $J = 4\times10^4$ mA/cm² (high injection level) with the measured slope [20, 21] of the (other

[21] J. S. Saby, Rep. Meeting on Semiconductors, Rugby 1956, p. 39.

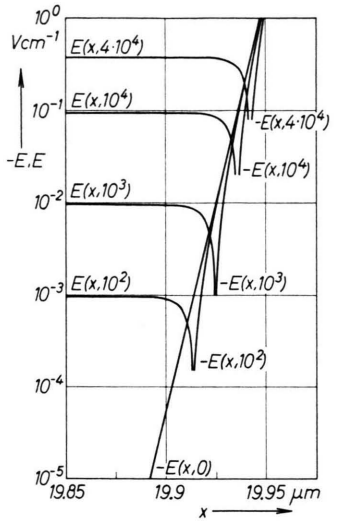

Fig. 5. Electric field distributions in the p region of Ge p^+-n junction diode, for values smaller than 1 V/cm, with total current density as parameter in mA/cm².

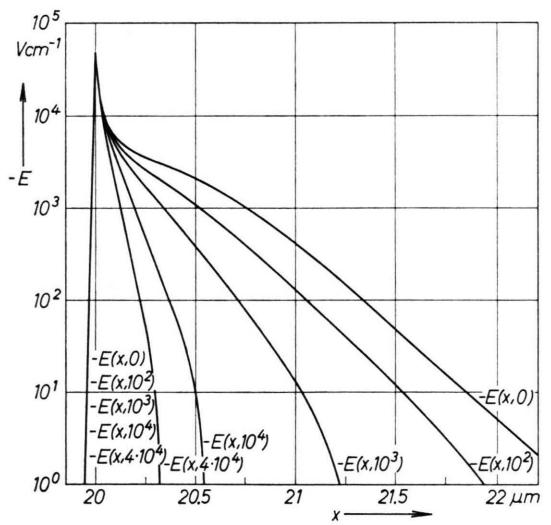

Fig. 6. Electric field distributions in the space-charge layer of Ge p^+-n junction diode, for values larger than 1 V/cm, with total current density as parameter in mA/cm².

broken) curve

$$J = \frac{4\times10^4}{261.94}\exp\left(\frac{e\,U_K}{2\,k\,T}\right)\mathrm{mA/cm^2}.$$

Fig. 16 shows also the limit between capacitive and inductive behaviour of alloyed germanium diodes (vertical broken line) which has been determined experimentally [20, 22] at about $U_K = 0.2$ V. The cor-

[22] G. Kohn, Arch. Elekt. Übertr. **9**, 241 [1955].

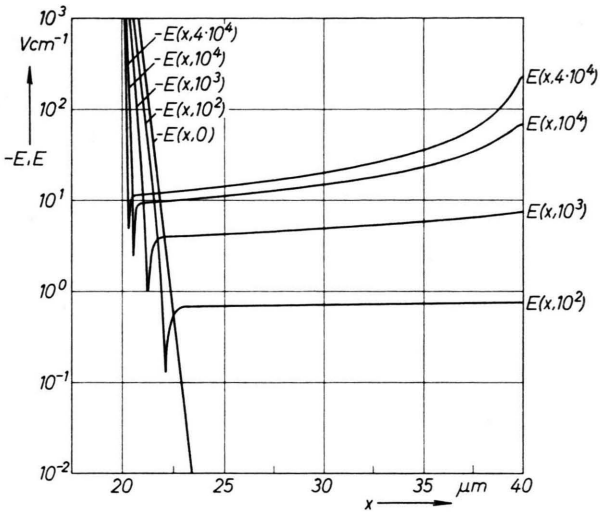

Fig. 7. Electric field distributions in the n region of Ge p⁺-n junction diode, for values smaller than 10^3 V/cm, with total current density as parameter in mA/cm² *.

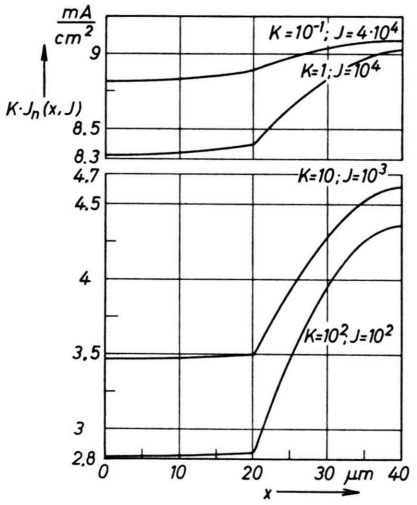

Fig. 8. Electron current density distributions in Ge p⁺-n junction diode with total current density J as parameter in mA/cm² and with K as dimensionless factor.

responding value of p obtained at $x = 22.2\ \mu$m (the so-called n side space-charge layer boundary) is found to be about $n_D = 4.6 \times 10^{14}/\text{cm}^3$ (compare Fig. 4), in accordance with values previously obtained [20, 23] by using simplified models.

* For $J = 10^3$ mA/cm² dE/dx also becomes equal to zero at $x = 40\ \mu$m (compare Ref. [16]).

[23] W. Guggenbühl, Arch. Elekt. Übertr. **10**, 483 [1956].

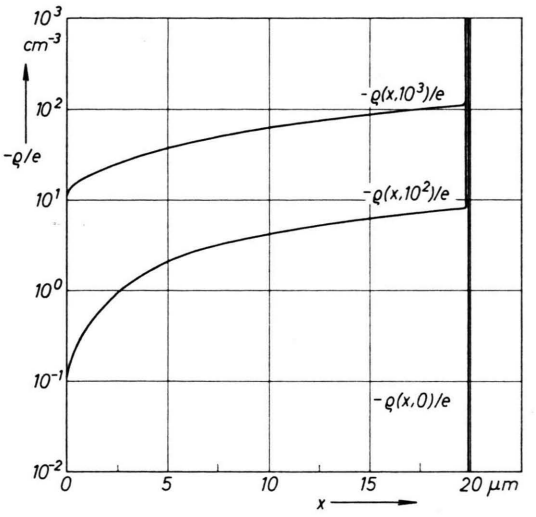

Fig. 9. Net charge density distributions in the p region of Ge p⁺-n junction diode, for values smaller than 10^3 cm^{-3}, with total current density as parameter in mA/cm².

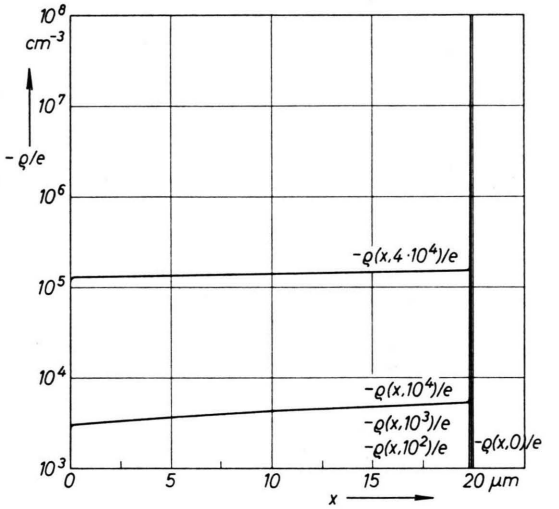

Fig. 10. Net charge density distributions in the p region of Ge p⁺-n junction diode, for values between 10^3 and 10^8 cm^{-3}, with total current density as parameter in mA/cm².

5. Test of the Computer Program and Comparison with the Schottky Approximation for $J = 0$

The system of differential Eqs. (1) – (5) has, for $J = 0$, the following closed analytical solutions:

$$J_p = 0\,, \tag{22}$$

$$J_n = 0\,, \tag{23}$$

$$p\,n = n_i^2\,, \tag{24}$$

$$p = \exp\{(-U + C)\, e/k\,T\}\,, \tag{25}$$

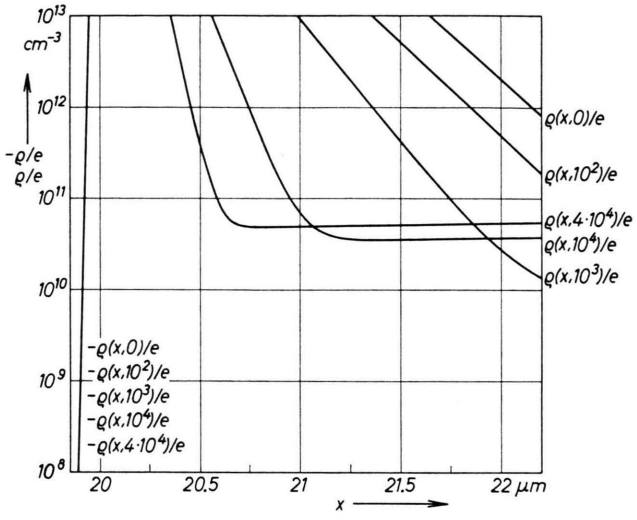

Fig. 11. Net charge density distributions in the space-charge layer of Ge p$^+$-n junction diode, for values between 10^8 and 10^{13} cm^{-3}, with total current density as parameter in mA/cm^2.

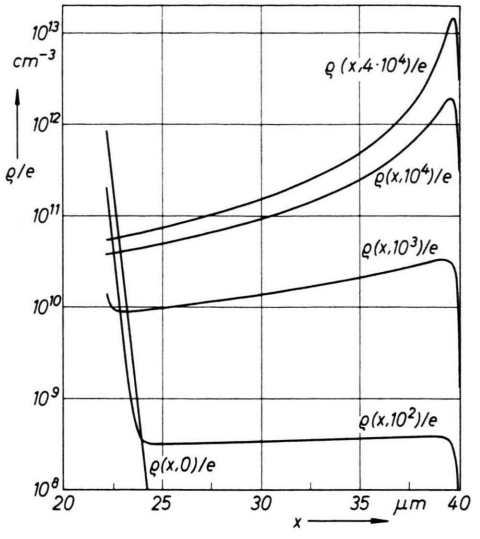

Fig. 13. Net charge density distributions in the quasineutral n region of Ge p$^+$-n junction diode with total current density as parameter in mA/cm^2.

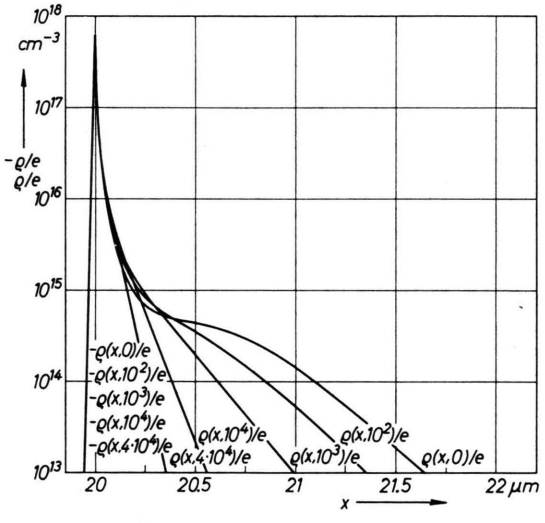

Fig. 12. Net charge density distributions in the space-charge layer of Ge p$^+$-n junction diode, for values larger than 10^{13} cm^{-3}, with total current density as parameter in mA/cm^2.

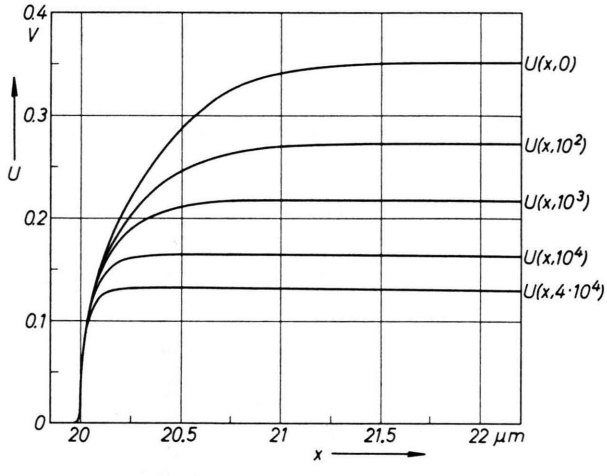

Fig. 14. Electrostatic potential distributions in the space-charge layer of Ge p$^+$-n junction diode with total current density as parameter in mA/cm^2.

where C is a constant of integration.

These solutions were numerically obtained for $J=0$ with the same computer program used for $J>0$ and with a relative numerical error smaller than 10^{-5} (compare Figs. 1, 2, 3, 4, 14 and 15 for $J=0$). This limit value was also the largest relative discretisation error of each integration step [24].

When the contribution of the mobile charges to the electric field in the space-charge layer of the p-n junction is neglected, following the approximation of SCHOTTKY [25] for a metal-semiconductor junction, the electric field at the abrupt transition of the doping profile becomes then [20]

$$-E|_{x=x_{ab}} = \sqrt{2\,\frac{e}{\varepsilon}\,(U_D - U_K)\,\frac{n_A\,n_D}{n_A+n_D}}\,, \qquad (26)$$

[24] Eqs. (22) to (25) represent the only closed analytical solutions with physical meaning under non-degenerate conditions. A test of the computer program, by comparison with the theory in Ref. [1], is, therefore, not possible for bias conditions other than equilibrium (see section 6).

[25] W. SCHOTTKY, Z. Phys. **118**, 539 [1942].

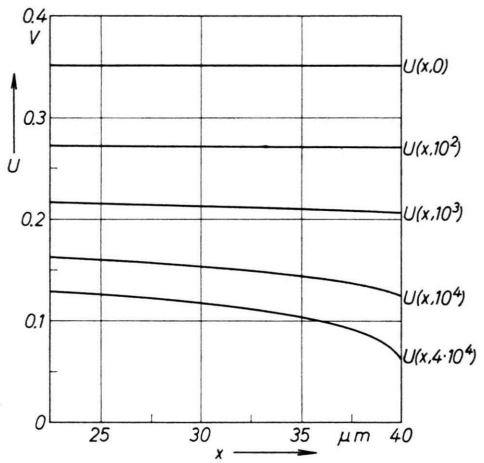

Fig. 15. Electrostatic potential distributions in the quasi-neutral n region of Ge p^+-n junction diode with total current density as parameter in mA/cm².

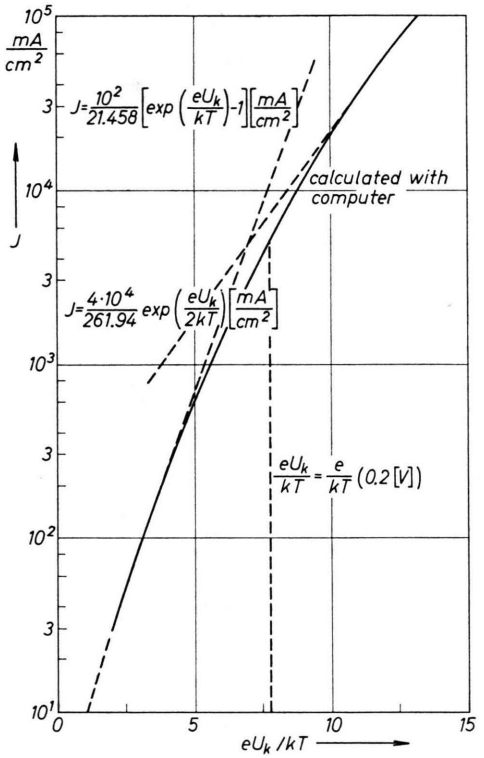

Fig. 16. Forward current/voltage characteristic of Ge p^+-n junction diode.

and the part of the space-charge layer in the n material is given by

$$x_n - x_{ab} = -E|_{x=x_{ab}} \frac{\varepsilon}{e\, n_D}, \tag{27}$$

where U_D is the diffusion voltage.

By applying Eqs. (26) and (27) to the p-n junction considered here, the following values are obtained for $J=0$:

$$-E|_{x=x_{ab}} = 6.04 \times 10^3 \text{ V/cm}, \quad x_n - x_{ab} = 1.16\ \mu\text{m},$$

which are not in agreement with the results in Figs. 6 and 7, since the hole concentration is at $x = x_{ab} = 20\ \mu$m from the same order of magnitude of n_A in the p region.

6. Comparison with the Shockley Theory for $J = 10^2$ mA/cm²

With the assumptions of the SHOCKLEY theory of a p-n junction [1], the following solution of the boundary-value problem is obtained in the p region:

$$n = \frac{n_p[\exp(e\,U_K/k\,T)-1]}{\sinh(x_p/L_n)} \sinh(x/L_n) + n_p, \tag{28}$$

$$J_n = e\,D_n \frac{n_p[\exp(e\,U_K/k\,T)-1]}{L_n \sinh(x_p/L_n)} \cosh(x/L_n). \tag{29}$$

The similar solution in the n region is:

$$p = \frac{p_n[\exp(e\,U_K/k\,T)-1]}{\sinh[(x_1-x_n)/L_p]} \sinh[(x_1-x)/L_p] + p_n, \tag{30}$$

$$J_p = e\,D_p \frac{p_n[\exp(e\,U_K/k\,T)-1]}{L_p \sinh[(x_1-x_n)/L_p]} \cosh[(x_1-x)/L_p]. \tag{31}$$

The expression for the direct current becomes then

$$J = e\left[\frac{n_p D_n}{L_n}\operatorname{cotgh}\left(\frac{x_p}{L_n}\right) + \frac{p_n D_p}{L_p}\operatorname{cotgh}\left(\frac{x_1-x_n}{L_p}\right)\right] \cdot [\exp(e\,U_K/k\,T)-1] = J_0[\exp(e\,U_K/k\,T)-1], \tag{32}$$

where

$L_n = \sqrt{D_n \tau_{n0}}$,
$L_p = \sqrt{D_p \tau_{p0}}$,
$x = 0$ at the p side contact,
$x = x_1$ at the n side contact,
x_p = p side boundary of the space-charge layer,
x_n = n side boundary of the space-charge layer,
n_p = asymptotic value of n in an infinitely long p region.

The values of x_p and x_n cannot be obtained from the theories in Ref. [1] and [25]. However, in order to compare the SHOCKLEY theory [1] with the "exact" solution obtained here for $J = 10^2$ mA/cm², the following values of U_K and x_p are used:

$U_K = 0.08041$ V: the value of U_K for which $J = 10^2$ mA/cm², according to the computed characteristic in Fig. 16;

$x_p = 19.93\ \mu m$: the value of x for which Eq. (28) gives, for $x = x_p$, the "exact" computed value of n.

The comparison is then made for the following three values of x_n:

(a) $x_n = 25\ \mu m$: the value of x at the minimum of the space-charge density, according to Fig. 13. In this case, the curve 1 in Fig. 17 is obtained from Eq. (30) instead of the "exact" full curve in the same figure. Eq. (32) gives then $J_0 = 6.18\ mA/cm^2$ instead of $(10^2/21.458)\ mAcm^{-2} = 4.66\ mAcm^{-2}$, conforming to Fig. 16.

(b) $x_n = 22.12\ \mu m$: the value of x at the change of sign of E, according to Fig. 7. From Eq. (30) the curve 2 in Fig. 17 is then obtained. Eq. (32) leads, in this case, to $J_0 = 5.18\ mA/cm^2$.

(c) $x_n = 21.095\ \mu m$: the value of x for which Eq. (30) gives, for $x = x_n$, the "exact" computed value of p. From Eq. (30) the curve 3 in Fig. 17 is then obtained. Eq. (32) leads, in this case, to $J_0 = 4.90\ mA/cm^2$. According to Eq. (31), J_p is nearly constant in the n region and becomes $J_p = 105\ mA/cm^2$ instead of the distribution of $J - J_n$ which can be obtained from Fig. 8.

In the p region J_n is, according to Eq. (29), nearly constant for the three cases considered and becomes $J_n = 2.82 \times 10^{-2}\ mA/cm^2$ instead of the distribution in Fig. 8. The distribution of n, obtained from Eq. (28), agrees for $0 \leqq x \leqq x_p$ up to 0.1% with the "exact" distribution.

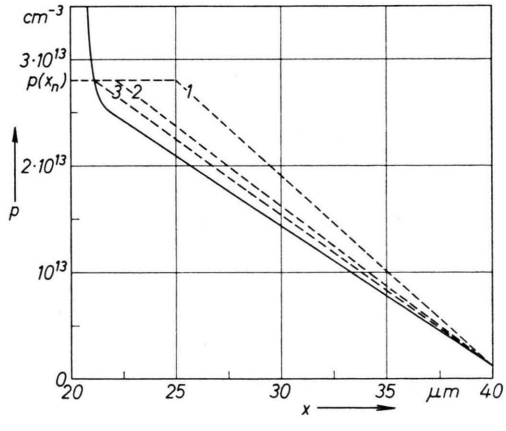

Fig. 17. Minority carrier concentration distributions in the quasineutral n region of Ge p^+-n junction diode for $J = 10^2\ mA/cm^2$. Full curve: "Exact" distribution. Broken curves: Distributions according to the SHOCKLEY theory for three "possible" values of the space-charge layer boundary.

7. On the Dependence of Mobility on Carrier Temperature in the p – n Junction

The present solution has been obtained under the assumption of uniform electron temperature T_n, hole temperature T_p and lattice temperature T, with $T_n = T_p = T = 300\ ^\circ K$. The mobilities μ_n and μ_p have been then considered as uniform quantities between each electrode and the abrupt transition of the doping profile, by taking into account the acoustical and optical mode scattering and the ionized impurity scattering.

For a nonuniform electric field distribution, as it is the case in a p-n junction, T_n, T_p and T become nonuniform and are to be considered as further dependent variables. The mobilities also become nonuniform and a more generalized system of differential equations [16] is then to be integrated. For forward bias, however, the carriers are heated only in the quasineutral p and n regions of the p-n junction and μ_n and μ_p, for the case considered, are constant up to the maximum of E obtained in these regions (compare Figs. 5 and 7 and Ref. [15]). This justifies the assumption made.

On the other hand, the relaxation times τ_n for electrons and τ_p for holes are then uniform between each electrode and the abrupt transition of the doping profile, since this is the case for the doping profile and the lattice temperature. The terms with $\partial\tau_n/\partial x$ and $\partial\tau_p/\partial x$ can be omitted in the expressions generalized in Ref. [8] for the electron and hole current. This leads, with the assumption mentioned above, to Eqs. (1) and (2).

Acknowledgments

The author would like to express his gratitude to Prof. Dr. M. J. O. STRUTT, Head of the Department of Advanced Electrical Engineering, for his guidance and encouragement during this research. Thanks are also due to Prof. Dr. E. STIEFEL and Dir. A. SCHAI for permission to use the Control Data 1604-A computer. This work was supported by the Swiss Federal Fund for the Advancement of Economy, by the Swiss National Science Foundation and by the Centenary Fund of the Swiss Federal Institute of Technology.

Appendix

1. Some Properties of the Characteristics

The Figures 18 and 19 show the $(y_1 - y_2)$, y_1-projections and the y_4, y_1-projections of 14 computed characteristics of the autonomous system of

differential Eqs. (1) – (5) for $J=10^3$ mA/cm². The values of the constants conform to section 1 for $20\ \mu m \leqq x \leqq 40\ \mu m$. The y_4, y_1-projection of each characteristic extends to the same value of y_1 as the (y_1-y_2), y_1-projection. The y_3, y_1-projections of these characteristics, extended also to the same values of y_1, differ from the straight line $y_3=0.9983\times10^3$ mA/cm² by less than 0.0002×10^3 mA/cm² and are, therefore, not plotted.

All the 14 characteristics represented have the same initial values of $(-y_1+y_2)$ and $y_3{}^*$ at $y_1=0$. Only the initial value of

$$\mathrm{d}(-y_1+y_2)/\mathrm{d}y_1=-\mathrm{d}(\varrho/e)/\mathrm{d}(p-p_n)$$

at $y_1=0$ varies from one to another characteristic. This initial value increases from the characteristic phys_1 to the phys_7, from the phys_7 to the math_7 and from the math_7 to the math_1. Already for the characteristics phys_3 and math_3 the initial values of $\mathrm{d}(-y_1+y_2)/\mathrm{d}y_1$ differ relatively by less than 10^{-10}. The parameter $\mathrm{d}(-y_1+y_2)/\mathrm{d}y_1\,|_{y_1=0}$ varies, therefore, within a very small interval around the value corresponding to the characteristic phys_7, whose trajectories satisfy the boundary and continuity conditions, conforming to section 1.

As it appears from the Figures 18 and 19, two kinds of characteristics are to be distinguished:

(a) the characteristics, such as the phys_1 to phys_7, in which the sign of ϱ/e does not change and which can be physically meaningful;

(b) the characteristics, such as the math_1 to math_7, in which the sign of ϱ/e changes and which are, therefore, only mathematically meaningful.

All the characteristics computed to solve the boundary-value problem for $J=0$, $J=10^2$ mA/cm², $J=10^3$ mA/cm², $J=10^4$ mA/cm² and $J=4\times10^4$ mA/cm² present analog properties not only for $20\ \mu m \leqq x \leqq 40\ \mu m$ but also for $0 \leqq x < 20\ \mu m$.

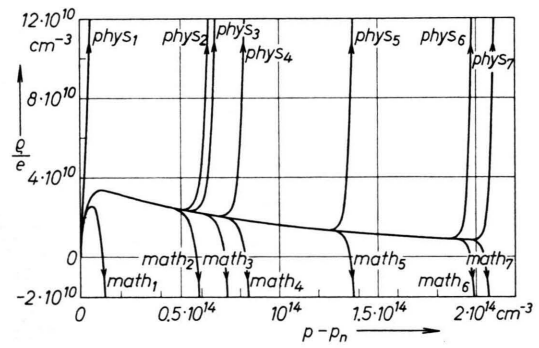

Fig. 18. (y_1-y_2), y_1-projections of 14 computed characteristics corresponding to trajectories in the n region of Ge p^+-n junction diode, for $J=10^3$ mA/cm², with $\mathrm{d}(-y_1+y_2)/\mathrm{d}y_1\,|_{y_1=0}$ as parameter.

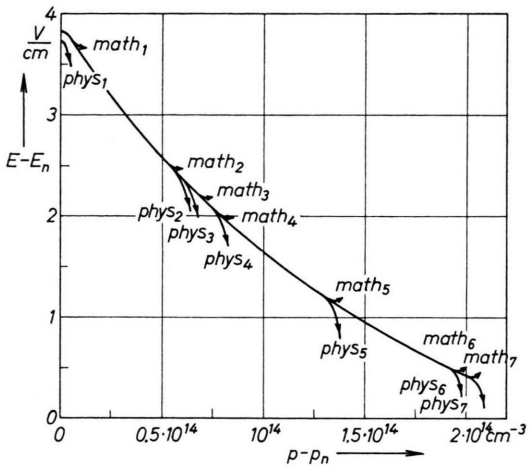

Fig. 19. y_4, y_1-projections of the characteristics represented in Fig. 18, extended to the same values of y_1.

2. *Determination of the Unknown Initial Values of the Trajectories*

The values of the unknown magnitudes

$$\mathrm{d}p/\mathrm{d}x\,|_{x=40\ \mu m} \quad \text{and} \quad \mathrm{d}n/\mathrm{d}x\,|_{x=40\ \mu m}$$

corresponding to the trajectories which satisfy the boundary and continuity conditions, conforming to section 1, can be determined in a relatively easy way thanks to the above special properties of the characteristics. Because of these properties and of the relation

$$\frac{\mathrm{d}n/\mathrm{d}x\,|_{x=40\ \mu m}}{\mathrm{d}p/\mathrm{d}x\,|_{x=40\ \mu m}}=1-\left.\frac{\mathrm{d}(\varrho/e)}{\mathrm{d}y_1}\right|_{y_1=0}$$

the variability field of the possible pair of guesses of $\mathrm{d}p/\mathrm{d}x\,|_{x=40\ \mu m}$ and $\mathrm{d}n/\mathrm{d}x\,|_{x=40\ \mu m}$ in the $\mathrm{d}p/\mathrm{d}x\,|_{x=40\ \mu m}$, $\mathrm{d}n/\mathrm{d}x\,|_{x=40\ \mu m}$ – plane reduces to a narrow strip. For each guess of $\mathrm{d}p/\mathrm{d}x\,|_{x=40\ \mu m}$ there is a very small variability interval of the guess of $\mathrm{d}n/\mathrm{d}x\,|_{x=40\ \mu m}$, which is determined by an iteration process. With this iteration process a one-parameter family of characteristics, such as the 14 characteristics represented in the Figures 18 and 19, is calculated by varying the guess of $\mathrm{d}n/\mathrm{d}x\,|_{x=40\ \mu m}$ so that the (y_1-y_2), y_1-projection of each new computed characteristic lies between the projections of the two last computed characteristics of different kind (as defined in section 1 of this appendix). The iteration pro-

cess is repeated for various guesses of $dp/dx|_{x=40\,\mu m}$ until a strip of points $(dp/dx|_{x=40\,\mu m}, dn/dx|_{x=40\,\mu m})$ with the corresponding trajectories in the n region of the p-n junction is obtained.

With the above method another strip of points $(dn/dx|_{x=0}, dp/dx|_{x=0})$ in the $dn/dx|_{x=0}, dp/dx|_{x=0}$-plane with the corresponding trajectories in the p region is also obtained. By comparison of the values of the obtained trajectories in both regions of the p-n junction at $x=20\ \mu m$, a smaller field in the $dp/dx|_{x=40\,\mu m}, dn/dx|_{x=40\,\mu m}$-plane and another in the $dn/dx|_{x=0}, dp/dx|_{x=0}$-plane are determined, in which the unknown initial values are contained.

In the new smaller fields the density of points is increased, the corresponding additional characteristics are then computed, and the comparison is again made in order to obtain much smaller fields with the unknown initial values. The process is repeated until the trajectories in the n and p regions of the p-n junction satisfy the continuity conditions at $x=20$ μm with a relative error smaller than 0.2%.

For $J=0$ the two strips of points $(dp/dx|_{x=40\,\mu m}, dn/dx|_{x=40\,\mu m})$ and $(dn/dx|_{x=0}, dp/dx|_{x=0})$ reduce, because of Eq. (24), to the straight lines

$$\frac{dn/dx|_{x=40\,\mu m}}{dp/dx|_{x=40\,\mu m}} = -\frac{n_n}{p_n}$$

and

$$\frac{dp/dx|_{x=0}}{dn/dx|_{x=0}} = -\frac{p_p}{n_p}$$

respectively, where p_p is the asymptotic value of p in an infinitely long p region.

The computer program used (in ALGOL 60) is fully described in Ref. [16], which includes further details concerning the numerical procedure applied in order to avoid the use of subprograms for the computation with multiple precision.

Zur Bandstruktur von Wismuttellurid*

P. DRATH

Mitteilung aus der Physikalisch-Technischen Bundesanstalt, Braunschweig

(Z. Naturforsch. **23 a**, 1146—1154 [1968]; eingegangen am 21. Mai 1968)

The analysis of Shubnikov-De Haas oscillations in n- and p-type Bi_2Te_3 indicate the existence of a multivalley structure of valence and conduction band. In p-type Bi_2Te_3 the surfaces of constant energy are found to consist of 6 ellipsoids. Spin splitting of the Landau-levels was observed, the anisotropy of the g-factor in the trigonal-bisectrix plane is consistent with an existing theory. In n-type Bi_2Te_3 Hall-coefficient, magnetoresistance and g-factor do not follow the predicted pattern of a simple many valley model, so that the number of ellipsoids could not be determined with certainty. The presence of an additional band must be considered.

Für das Leitungs- und Valenzband von Wismuttellurid (Kristallklasse $R\bar{3}m$) wurde von DRABBLE und WOLFE [1] ein Vieltälermodell vorgeschlagen. Danach sollen die Energieextrema in den Spiegelebenen des reziproken Gitters liegen. Die Flächen gleicher Energie im k-Raum sollen Ellipsoide sein, wobei 3 Ellipsoide zu erwarten sind, wenn ihre Mittelpunkte auf den Begrenzungsflächen der Brillouin-Zone liegen, und sonst 6 Ellipsoide. Für sphärische und ellipsoidförmige Energieflächen kann der Zusammenhang zwischen der Energie und dem Wellenzahlvektor in folgender Form geschrieben werden:

$$E = (\hbar^2/2m_0)\, \boldsymbol{k}^+ \boldsymbol{\alpha}\, \boldsymbol{k}. \qquad (1)$$

Dabei ist m_0 die Masse des freien Elektrons, $\boldsymbol{k}^+$ bezeichnet die transponierte Matrix. E rechnet von der Bandkante aus. Der Abstand des Energieextremums vom Nullpunkt des Koordinatensystems im k-Raum wird dabei nicht berücksichtigt. $\boldsymbol{\alpha}$ ist der Tensor der reziproken effektiven Masse:

$$\boldsymbol{\alpha} = (\boldsymbol{m}^*)^{-1}.$$

In dem von Drabble und Wolfe vorgeschlagenen Modell hat $\boldsymbol{\alpha}$ vier Komponenten

$$\alpha_{11},\ \alpha_{22},\ \alpha_{33} \text{ und } \alpha_{23},$$

dabei bezeichnen 1, 2 und 3 die Richtungen parallel zu einer binären Achse, zu einer Bisektrix und zur

* Auszug aus der Dissertation des Verfassers, Technische Hochschule Braunschweig 1967.

[1] J. R. DRABBLE u. R. WOLFE, Proc. Phys. Soc. London **69**, 1101 [1956].